IEEE Photonics Journal
An IEEE Photonics Society Publication

Open Access

Symmetric Step-Apodized Distributed Feedback Fiber Laser With Improved Efficiency

Volume 11, Number 4, August 2019

Kuikui Guo
Jun He
Kaiming Yang
Zhe Zhang
Xizhen Xu
Bin Du
Gaixia Xu
Yiping Wang, *Senior Member, IEEE*

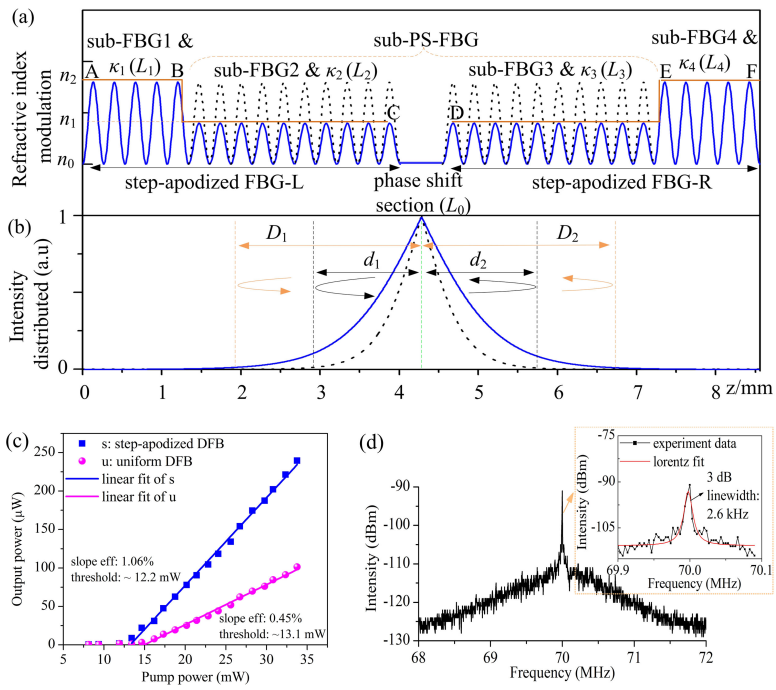

DOI: 10.1109/JPHOT.2019.2921628
1943-0655

Symmetric Step-Apodized Distributed Feedback Fiber Laser With Improved Efficiency

Kuikui Guo,[1,2] Jun He,[1,2] Kaiming Yang,[1,2] Zhe Zhang,[1,2] Xizhen Xu,[1,2] Bin Du,[1,2] Gaixia Xu,[3] and Yiping Wang,[1,2] *Senior Member, IEEE*

[1]Key Laboratory of Optoelectronic Devices and Systems of Ministry of Education and Guangdong Province, College of Physics and Optoelectronic Engineering, Shenzhen University, Shenzhen 518060, China
[2]Guangdong and Hong Kong Joint Research Centre for Optical Fibre Sensors, Shenzhen University, Shenzhen 518060, China
[3]Guangdong Key Laboratory for Biomedical Measurements and Ultrasound Imaging, School of Biomedical Engineering, Health Science Center, Shenzhen University, Shenzhen 518055, China

DOI:10.1109/JPHOT.2019.2921628

Manuscript received April 6, 2019; revised May 30, 2019; accepted June 4, 2019. Date of publication June 7, 2019; date of current version June 28, 2019. This work was supported by the National Natural Science Foundation of China under Grant 61875128, Grant 91860138, and Grant 61635007, in part by the Science and Technology Innovation Commission of Shenzhen under Grant JCYJ20180507182058432, Grant JCYJ20160427104925452, and Grant GRCK2017082111254221, and in part by the Development and Reform Commission of Shenzhen Municipality Foundation. Corresponding author: Jun He (e-mail: hejun07@szu.edu.cn).

Abstract: We propose and demonstrate a symmetric step-apodized distributed feedback (DFB) fiber laser, which has an improved efficiency and a narrow linewidth. This special DFB laser cavity is based on a unique symmetric step-apodized π-phase-shifted fiber Bragg grating (FBG) directly inscribed in a heavily erbium-doped fiber. The symmetric step-apodized phase-shifted grating is equivalent to a weak uniform phase-shifted FBG embedded in a pair of strong FBGs, and this design could increase the effective cavity length of a DFB fiber laser. Moreover, the symmetric step-apodized DFB laser cavity proposed in this work has a phase shift located in the cavity center. It could simplify the design process significantly due to the symmetry in the laser cavity. Experimental results show that the slope efficiency of a symmetric step-apodized DFB fiber laser could be increased to 1.06%, which is significantly higher than that of a uniform DFB fiber laser (i.e., 0.45%) under the same cavity length and pump conditions. In addition, the proposed DFB fiber laser exhibits a high stability. The fluctuations in lasing wavelength and output power were less than 12 pm (corresponding to a frequency shift of 1.49 GHz) and 0.13 dB within 24 h, respectively. Moreover, the full-width at half-maximum linewidth of the symmetric step-apodized DFB fiber laser was $\sim$2.6 kHz, measured by the delayed self-heterodyne method with a 50-km fiber delayed line. As such, the proposed symmetric step-apodized DFB fiber laser could potentially be used as high-performance light source for fiber-optic sensors or coherent optical communication systems.

Index Terms: Lasers, fiber, lasers, distributed-feedback, fibers, erbium, fiber Bragg gratings, apodized.

1. Introduction

Over the past decades, distributed feedback (DFB) fiber lasers have a number of applications in coherent optical communications [1], fiber-optic sensors [2]–[4], and microwave signal generation [5] due to the advantages of single-mode operation, narrow linewidth, low noise, and high stability [6]–[9]. DFB fiber lasers are typically fabricated by optically pumping an active cavity consisting of a phase-shifted fiber Bragg grating (PS-FBG) inscribed directly in a section of rare-earth-doped fiber. The unique resonant cavities of these DFB fiber lasers provide a single-longitudinal-mode (single-frequency) laser output. However, the limited effective cavity length of a traditional DFB fiber laser will limit the absorption efficiency of pump power and hence results in a significant reduction in laser output power. The efficiency is a critical attribute for fiber lasers and the reduction in efficiency increases the required pump power [10]. Additionally, both the output power and efficiency could be improved by increasing the effective cavity length of fiber laser. For instance, distributed Bragg reflector (DBR) fiber lasers, which typically have a much longer cavity length, have been developed to improve the efficiency. However, in case the cavity length of DBR fiber laser is larger than a certain value, multiple longitudinal modes (multiple frequencies) will emerge in the DBR fiber laser output [11]. As a result, a new design of DFB fiber laser cavity is still in demand for improving the efficiency of single-frequency fiber lasers.

A variety of DFB fiber lasers have already been reported with different designs in the laser cavities, and these DFB fiber lasers offered different operational performance. For example, Kogelnik *et al*. proposed a DFB laser based on a uniform FBG with no phase shift or end reflectors. This device operated at two modes spaced symmetrically around the Bragg wavelength [12]. In 1995, Loh *et al*. reported an erbium-doped DFB fiber laser based on a uniform π-PS FBG, which had a permanent π phase shift at the FBG center, a constant refractive index modulation profile and a constant grating period [13]. This conventional DFB fiber laser cavity could produce a single-frequency operation. However, the output power of these DFB fiber lasers was limited by the pump absorption, gain medium saturation, and heat dissipation in a short and symmetric DFB laser cavity, and hence it was typically less than several mW [14]. Additionally, the excited-state absorption (ESA) process is also important as a source of extra loss in both pump wavelength and lasing wavelength, which noticeably limit the output efficiency of fiber laser [15]–[17].

Asymmetric DFB fiber lasers were studied to improve the laser efficiency. For example, Li *et al*. fabricated a DFB fiber laser using an asymmetric π-PS-FBG. They improved the output power from the shorter end by positioning the phase shift asymmetrically with respect to the FBG center [8]. However, it is difficult to determine the precise phase shift position in this asymmetric design. Furthermore, an asymmetric step-apodized DFB fiber laser was reported to increase the efficiency at both ends of the DFB fiber laser [18]. The resonant cavity of the asymmetric step-apodized DFB fiber laser consisted of a special π-phase-shifted FBG, in which the left and right FBGs beside the phase-shifted section had different grating lengths and different coupling coefficients. In other words, there was a step change in the coupling coefficient on either side of the phase shift [18]. The laser output power could be maximized in such an asymmetric step-apodized DFB fiber laser. To date, various studies have been done to improve the efficiency of these DFB fiber lasers by optimizing the laser cavity and grating parameters, such as grating length, grating strength, phase shift value, and phase shift position. Nevertheless, it is quite complex and difficult to obtain the optimum grating parameters, including the coupling coefficients and grating lengths of each sub-FBG in phase-shifted FBG.

In this study, we propose and demonstrate a symmetric step-apodized DFB fiber laser with an improved efficiency and a narrow linewidth. This special DFB fiber laser cavity consists of a symmetric step-apodized π-PS-FBG directly inscribed in a section of erbium-doped fiber. The symmetric step-apodized phase-shifted grating could be equivalent to a weak uniform phase-shifted FBG embedded in a pair of strong FBGs, and this design could increase the effective length of the DFB fiber laser cavity. Experimental results show that the slope efficiency of a symmetric step-apodized DFB fiber laser could be increased to 1.06% and is much higher than that of a uniform DFB fiber laser under the same cavity length and pump conditions. In addition, this DFB fiber laser exhibited a high stability and a narrow linewidth. The proposed DFB fiber laser typically operated

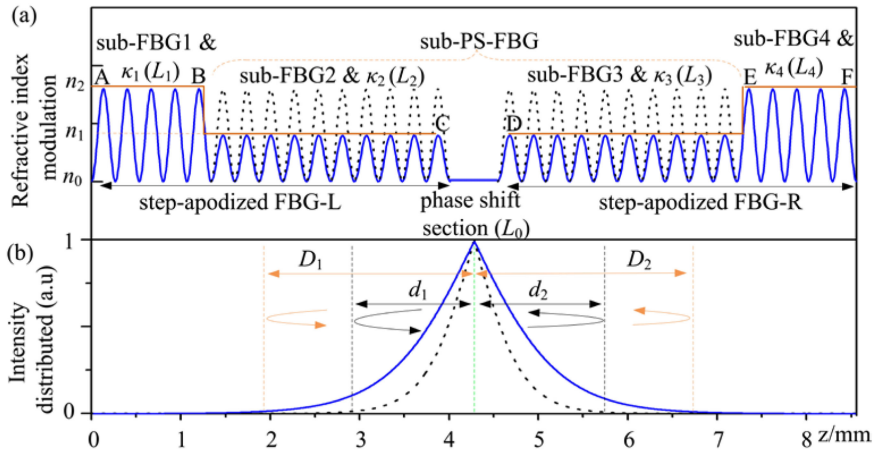

Fig. 1. An illustration of (a) refractive index modulation and (b) normalized intensity distribution in a symmetric step-apodized PS-FBG and a uniform PS-FBG along the z direction; Note that the grating period has been exaggerated 498 times for clarity.

in two orthogonal polarization modes, whereas it could also operate in a single polarization mode using a side-polishing technique. Hence, the proposed symmetric step-apodized DFB fiber laser might be used as high-performance light source for fiber sensors or communication systems.

2. Theoretical Modeling and Analysis

The FBGs in this work were inscribed with UV exposure through a uniform phase mask. The refractive index in the fiber core of these FBGs varies sinusoidally along the fiber direction. The amplitude of the refractive index modulation in these FBGs could be flexibly changed by altering the UV laser exposure doze. As a result, we could create symmetric step-apodized PS-FBGs. Fig. 1(a) demonstrates the refractive index modulation profile of the proposed symmetric step-apodized PS-FBG of the DFB fiber laser. In order to analyze and optimize the grating structure, we divide the step-apodized PS-FBG into five parts, i.e., sub-FBG1, sub-FBG2, phase shift section, sub-FBG3, and sub-FBG4. Sub-FBG1 and sub-FBG4 have the same refractive index modulation amplitude n_2, whereas sub-FBG2 and sub-FBG3 have the same refractive index modulation amplitude n_1, which is smaller than n_2. Hence, the symmetric step-apodized PS-FBG is equivalent to a weak uniform sub-PS-FBG embedded in a pair of strong sub FBGs, i.e., sub-FBG1 and sub-FBG2, as shown in Fig. 1(a). Moreover, the refractive index modulation profile of a uniform PS-FBG of the DFB fiber laser is also demonstrated in Fig. 1(a) for comparison. Note that the grating period has been exaggerated 498 times for clarity.

Fig. 1(b) illustrates the normalized laser intensity distribution inside the proposed DFB fiber laser with a symmetric step-apodized PS-FBG and a DFB fiber laser with a uniform PS-FBG. It could be seen high intra-cavity power concentrated around the phase shift region. Fields propagating to the left and right are trapped by two grating segments, i.e., FBG-L and FBG-R, as shown in Fig. 1(a). They are circulating within a short cavity with the effective length, leading to the high intra-cavity laser power around the phase shift region.

Each grating segment on either side of the phase shift can be considered as a separate reflector. The reflection coefficient of the grating with a constant gain at the Bragg wavelength is given by [19], [20]:

$$r = \frac{-\kappa \sinh(\gamma L)}{\gamma \cosh(\gamma L) - g \sinh(\gamma L)}, \tag{1}$$

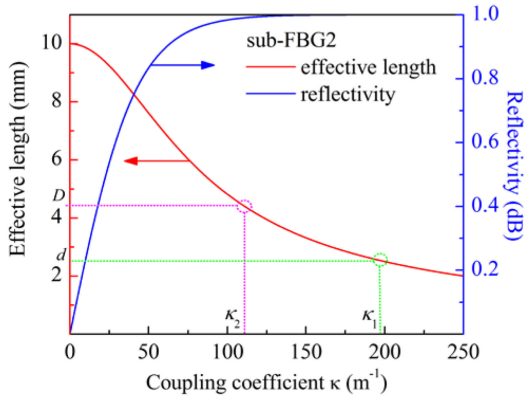

Fig. 2. The effective length and reflectivity of the sub-FBG2 with various coupling coefficients in the symmetric step-apodized PS-FBG.

where g is the field gain, κ is the coupling coefficient, L is the length of the grating, and $\gamma = \sqrt{\kappa^2 + g^2}$. In most practical applications, if g is small compared to κ, Eq. (1) can be simplified to:

$$r = -\tanh(\kappa L); g = \kappa. \tag{2}$$

In this case, the reflectivity R of the grating is given by:

$$R = \left|r^2\right| \approx \tanh^2(\kappa L). \tag{3}$$

The PS-FBG equals to a short fiber Fabry-Perot cavity, which includes a pair of FBGs [21]. The incident wave penetrates into the grating and the effective distance D is defined as the effective length of the grating, which can be expressed as [15]:

$$D = \frac{gL\left(\frac{\tanh(\gamma L)}{\gamma L} - \frac{1}{\cosh^2(\gamma L)}\right) + \tanh^2(\gamma L)}{g\tanh^2(\gamma L) + \gamma\tanh(\gamma L)}. \tag{4}$$

However, if $g \ll \kappa$, the effective length D of a grating can be approximated by:

$$D \approx \frac{\tanh(\kappa L)}{2\kappa} = \frac{|r|}{2\kappa}. \tag{5}$$

It could be seen from Eq. (5) that the effective lengths (i.e., 0.0025 mm) of the stronger sub-FBG1 and sub-FBG4 are negligible when coupling coefficient and grating length are 198.4 m^{-1}, 4 mm, respectively. Here, we only analyzed the effective length and reflectivity of the sub-FBG2 because the sub-FBG3 was equivalent to sub-FBG2. From Eq. (3) and Eq. (5), we can obtain the effective length and reflectivity of the sub-FBG2 as a function of the coupling coefficient κ for a given grating length of 20 mm, as shown in Fig. 2. It is obvious that the grating reflectivity decreases in case the effective length of sub-FBG2 is increased from κ_1 to κ_2, leading to a decrease in the optical feedback of the fiber laser cavity. However, the employment of the sub-FBG1 and sub-FBG4, which have a higher coupling coefficient, could maintain a sufficient grating reflectivity in the overall PS-FBG structure.

As such, we adopted a symmetric step-apodized PS-FBG, and this symmetric design could also negate the effects of phase shift position. In the case of a symmetric step-apodized PS-FBG and a uniform PS-FBG, as shown in Fig. 1(a), the total effective cavity length l_{eff} can be expressed as:

$$\begin{aligned} l_{eff} &= \frac{\tanh(\kappa_2 L_2)}{2\kappa_2} + L_0 + \frac{\tanh(\kappa_3 L_3)}{2\kappa_3} \\ &= \begin{cases} \frac{\tanh(\kappa_1 L_2)}{\kappa_1} + L_0, & \kappa_1 = \kappa_2 = \kappa_3,\ L_2 = L_3. \\ \frac{\tanh(\kappa_2 L_2)}{\kappa_2} + L_0, & \kappa_1 \neq \kappa_2 = \kappa_3,\ L_2 = L_3. \end{cases} \end{aligned} \tag{6}$$

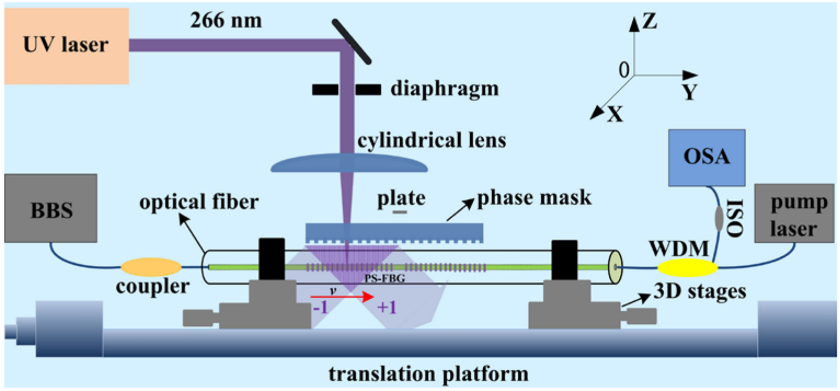

Fig. 3. A schematic diagram of the PS-FBG inscription process (BBS: broadband light source; OSA: optical spectrum analyzer; WDM: wavelength division multiplexer; ISO: isolator).

where L_2, L_0, and L_3 are the lengths of the sub-FBG2, phase shift section and sub-FBG3. κ_1, κ_2, and κ_3 are coupling coefficients. Equation (6) indicates that the effective cavity lengths of a uniform PS-FBG and a step-apodized PS-FBG could be determined from coupling coefficients κ_2 and κ_3. Hence, the total effective cavity length of the symmetric step-apodized fiber laser could be increased (i.e., $D_1 = D_2 > d_1 = d_2$) by decreasing coupling coefficients from κ_1 to κ_2, leading to an improved laser efficiency.

3. Fabrication of the Proposed Symmetric Step-Apodized DFB Fiber Laser

In this work, PS-FBGs were inscribed in a section of heavily-erbium-doped fiber (EDF, Nufern SM-ESF-7/125, peak absorption: 55 dB/m @ 1530 nm), which was loaded with hydrogen (80 °C and 13 MPa for 7 days) in advance to increase the fiber photosensitivity. The experimental setup used for fabricating PS-FBGs was similar to that presented in a previous work [22], [23]. A schematic diagram of the PS-FBG inscription process is shown in Fig. 3. Before the PS-FBG was inscribed, an EDF was spliced with two SMF and the splicing loss was less than 0.2 dB. The fabrication process can be described in detail as follows: a ~50 mW UV laser with a wavelength of 266 nm was focused using a cylindrical lens with a focal length of 50.2 mm. The beam was projected through a uniform phase mask (Ibsen Photonics, grating period: 1070 nm) onto the fiber core of the EDF. The ± 1 order diffraction beams were produced and an interference pattern with a period of 535 nm was created. This can induce periodic refractive index modulations when the fiber was exposed to the interference section. In this experiment, a plate was located 2 cm in front of the phase mask to shield the fiber from UV laser exposure. The phase mask and fiber were installed on a high-precision translation platform and were displaced perpendicular to the focused laser beam. The translation of the phase mask and fiber was controlled automatically using a LabVIEW program. The PS-FBG was inscribed with a scanning velocity v, as illustrated in Fig. 3. Transmission spectra were measured simultaneously using a broadband light source (BBS) and an optical spectrum analyzer (OSA, Yokogawa AQ6370C) with an intrinsic wavelength resolution of 0.02 nm.

Experiments were then conducted to compare the performance of two different DFB fiber lasers based on a symmetric step-apodized PS-FBG and a uniform PS-FBG, respectively. The coupling coefficients of these FBGs were changed by altering the scanning velocity of the UV laser beam [19]. At first, we set the scanning velocity ν to 0.05 mm/s, a uniform π PS-FBG with $\kappa_1 = \kappa_2 = \kappa_3 = \kappa_4$ was inscribed in the EDF with a total length of 50 mm, a shielded phase-shifted section length of ~2 mm, and a central wavelength of 1550.94 nm. The optical spectrum of the uniform PS-FBG (A to F in Fig. 1) is shown in Fig. 4(a). It should be noted the phase-shifted transmission slit could not be observed in Fig. 4(a) due to the limited wavelength resolution (0.02 nm) of the OSA. Moreover, the transmission loss at the Bragg wavelength of the PS-FBG was measured to be

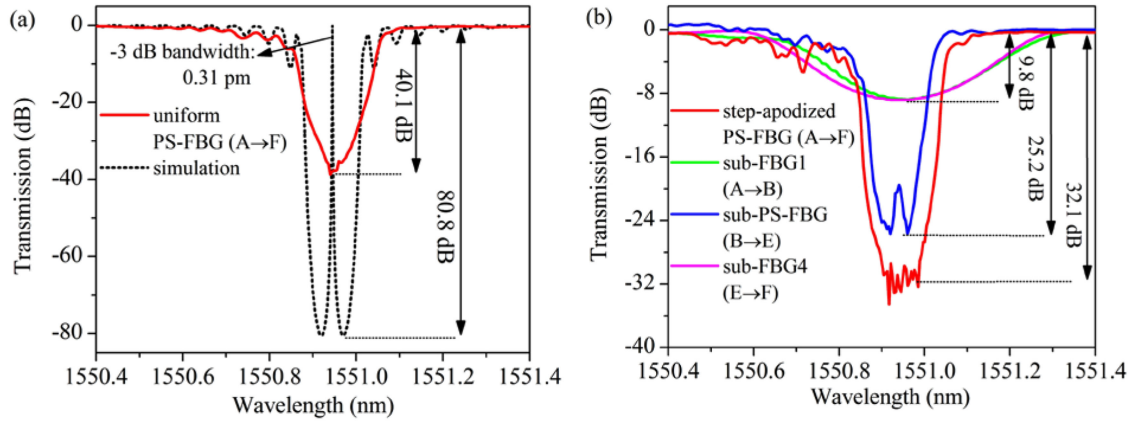

Fig. 4. (a) Optical spectra of the uniform PS-FBG on the EDF. (b) Optical spectra of the proposed symmetric step-apodized PS-FBG on the EDF and its sub-FBGs.

40.1 dB, which was also limited by the OSA resolution. The transmission spectrum of the uniform PS-FBG was calculated in MATLAB using the coupled-mode theory and a transfer matrix method [20], [24]. Simulation parameters included a fiber core refractive index of $n_0 = 1.447$, a grating period of $\Lambda = 535$ nm, and a coupling coefficient of 198.4 m^{-1}. These simulation results suggest that the phase-shifted transmission peak has a transmission loss of 80.8 dB, and a FWHM bandwidth (i.e., -3 dB bandwidth) of 0.31 pm. Subsequently, we fabricated a symmetric step-apodized PS-FBG and the corresponding transmission spectrum was shown in Fig. 4(b). The optical spectra of sub-FBGs during grating fabrication were also incorporated in Fig. 4(b). These transmission spectra were recorded separately in case the UV laser was scanned from A to B, B to E, and E to F to obtain the coupling coefficients of each sub gratings.

The fabrication process of the symmetric step-apodized DFB fiber laser can be described as follows. In step 1, the laser beam was scanned from A to B with a velocity of 0.05 mm/s as shown in Fig. 1, a sub-FBG1 with a length (L_1) of 4 mm, a high coupling coefficient of $\kappa_1 = 198.4$ m^{-1}, and a transmission loss of 9.8 dB at the Bragg wavelength was inscribed on the EDF. In step 2, the laser beam was scanned from B to E with a velocity of 0.1 mm/s, a sub-π-PS-FBG with a total length of 42 mm, a shielded phase-shifted section length of $\sim$2 mm, a low coupling coefficient of $\kappa_2 = \kappa_3 = 109.3$ m^{-1}, a central wavelength of 1550.94 nm, and a transmission loss of 25.2 dB at the Bragg wavelength was inscribed on the EDF. In step 3, the laser beam was scanned from E to F with a velocity of 0.05 mm/s, another sub-FBG4 with a length (L_4) of 4 mm, a high coupling coefficient of $\kappa_4 = 198.4$ m^{-1}, and a transmission loss of 9.8 dB at the Bragg wavelength was inscribed in the EDF. At last, the optical spectrum of step-apodized PS-FBG (A to F in Fig. 1) with a length of 50 mm, and a transmission loss of 32.1 dB is shown in Fig. 4(b). It could be seen from Fig. 4(b) that the phase-shifted peak wavelength of the sub-π-PS-FBG is slightly shorter than the Bragg wavelengths of the sub-FBG1 and sub-FBG4, resulting from the different coupling coefficients of these sub-gratings. Note that the step-apodized PS-FBG with high coupling coefficients at both ends could ensure a sufficient FBG reflectivity while increasing total effective cavity length of the device, which leads to an improved DFB fiber laser efficiency.

During the process in step 3, the optical spectrum of the step-apodized DFB fiber laser output was measured using a 980 nm pump laser diode together with a BBS, as shown in Fig. 3. The output from a pump laser operating at the wavelength of 980 nm was launched into the fiber laser cavity (i.e., the PS-FBG on EDF) through a wavelength division multiplexer (WDM), the isolator (ISO) was used to isolate the emitting laser that reflected from the fiber end face. As a result, the output performance of the DFB fiber laser was monitored in real time. Fig. 5(a) shows the optical spectrum evolutions when the sub-FBG4 was fabricated, i.e., the length of sub- FBG4 L_4 was increased from 0 to 4 mm as the UV laser beam was scanned on the EDF from E to F. It could

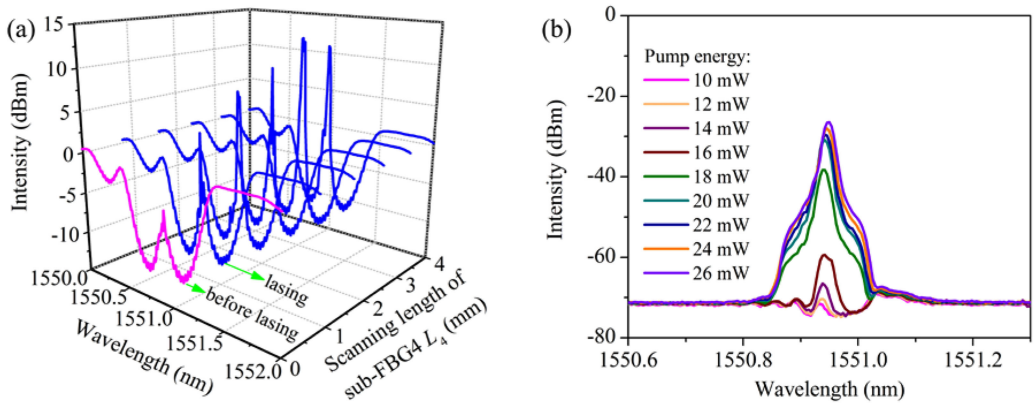

Fig. 5. (a) Optical spectrum evolutions of the symmetric step-apodized DFB fiber with an increasing length L_4 of the sub-FBG4. These results were measured with a pump laser and a BBS. (b) Optical spectrum evolutions of the symmetric step-apodized DFB fiber under increasing pump energy.

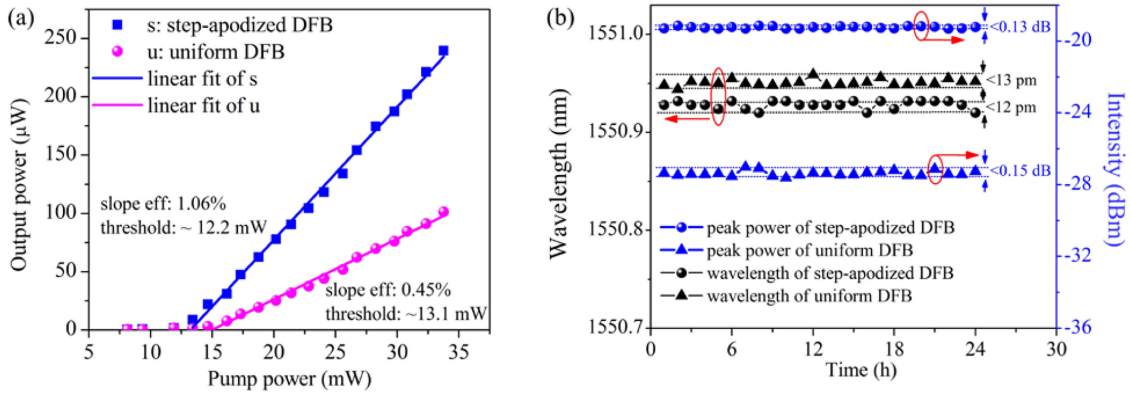

Fig. 6. (a) The output power of the step-apodized DFB fiber laser and the uniform DFB fiber laser as functions of the input pump power. (b) Stability of the lasing wavelength and Intensity of the step-apodized and uniform DFB fiber laser within 24 hours.

be seen the step-apodized DFB fiber laser began to oscillate in case L_4 was larger than 1.4 mm at fixed input pump energy of 50 mW. The result illustrates when the reflectivity of the sub-FBG4 gradually reached the reflectivity of the sub-FBG1, the phase shift value is approaching π and then the pump threshold and laser efficiency could be optimal [25]. Moreover, the grating inscription process terminated when the laser output power or SNR reaches its maximum. As a result, the total length of the symmetric step-apodized DFB fiber laser was 50 mm with the individual lengths of each sub-FBG and phase-shifted section are $L_1 = 4$ mm, $L_2 = 20$ mm, $L_0 = 2$ mm, $L_3 = 20$ mm, and $L_4 = 4$ mm, respectively. The optical spectrum evolutions of the symmetric step-apodized DFB fiber under various pump energy was shown in Fig. 5. It is obvious the laser intensity increases gradually and the lasing wavelength shifts towards longer wavelengths (i.e., a 'red' shift) with an increasing pump energy.

4. Results and Discussions

Fig. 6(a) illustrates the output power as functions of incident pump power for the proposed step-apodized DFB fiber laser and the uniform DFB fiber laser, respectively. The proposed symmetric step-apodized and uniform DFB fiber laser exhibit a threshold power of ~12.2 mW and ~13.1 mW,

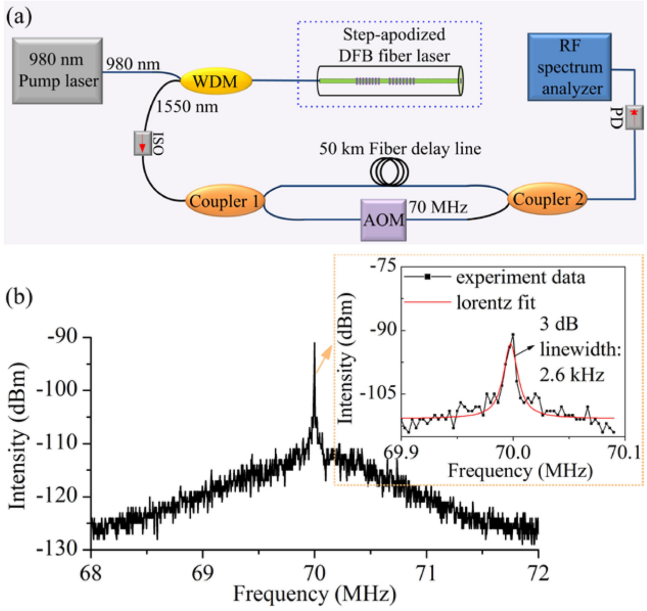

Fig. 7. (a) Schematic diagram of the proposed DFB fiber laser linewidth measurement system using delayed self-heterodyne (DSH) method. (b) The beat signal of the symmetric step-apodized DFB fiber laser output measured by DSH.

slope effective of ∼1.06% and 0.45%, respectively. In addition, the DFB fiber laser with a similar uniform structure reported previously exhibited a similar lower efficiency of 0.43% [23]. As such, the step-apodized DFB fiber achieved better output performance than the uniform DFB fiber laser, which is consistent with our theoretical analysis, i.e., increasing the effective cavity length of the DFB fiber laser by decreasing the grating coupling coefficient (while maintaining the sufficient reflectivity) could improve the laser output performance. Moreover, it should be noted that the asymmetric step-apodization design approach with an optimized phase-shift position could also improve the efficiency of DFB fiber lasers [18]. However, it is quite difficult to find the optimum parameters for such an asymmetric step-apodized DFB laser cavity. Nevertheless, the symmetric step-apodized DFB laser cavity proposed in this work has a phase shift located in the center of the grating. This could simplify the design process significantly due to the symmetry in laser cavity.

Fig. 6(b) demonstrates the output stability of a step-apodized DFB fiber laser and a uniform DFB fiber laser. The lasing wavelength and intensity of two DFB fiber lasers were recorded at 1 hour intervals within 24 hours. The results exhibit a very high stability in both lasing wavelength and intensity in both two types of DFB fiber lasers. For example, the fluctuations in lasing wavelength of the step-apodized and the uniform DFB fiber lasers are less than 12 and 13 pm, corresponding to a frequency fluctuation of 1.49 and 1.62 GHz, respectively. Moreover, the intensity fluctuations of the step-apodized and the uniform DFB fiber lasers are 0.13 and 0.15 dB, respectively.

Furthermore, the linewidth characteristic of the proposed step-apodized DFB fiber laser was also investigated using a conventional delayed self-heterodyne (DSH) method [26], [27]. The experimental setup is shown in Fig. 7(a). The output from a pump laser diode (LD) operating at a wavelength of 980 nm was launched into the fiber laser cavity (i.e., the step-apodized PS-FBG in the EDF) through a wavelength division multiplexer (WDM). An isolator (ISO) between the WDM and coupler1 was used to isolate the backward transmitted signal. The DSH technique was employed by connecting the DFB fiber laser output into the coupler 1, which divided the signal into two arms. One arm was sent through a 50 km fiber delay line, producing a delay time of ∼250 μs. The other arm was connected to an acousto-optic modulator (AOM) with a carrier frequency shift of 70 MHz. Coupler 2 was used to recombine the two arms beams and the heterodyne signal was

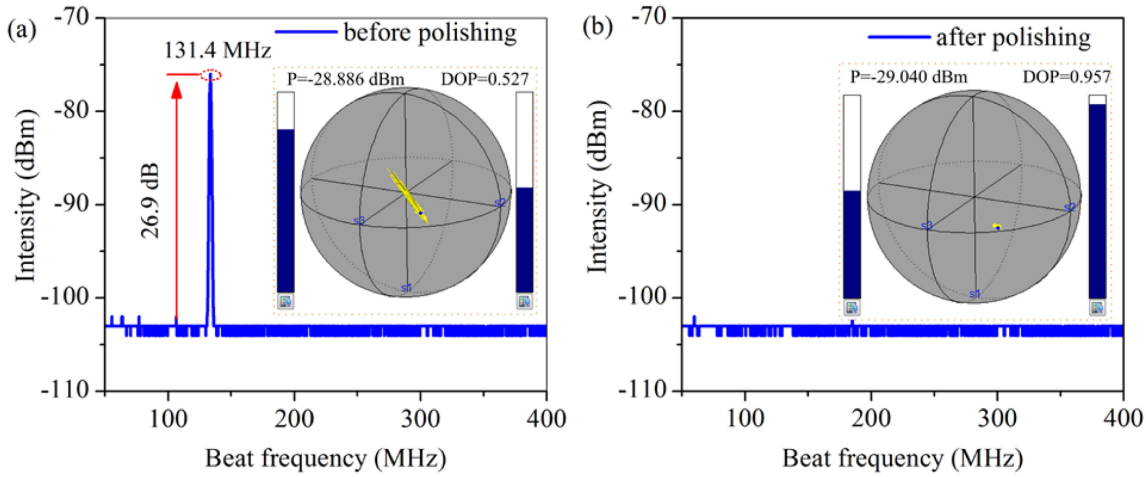

Fig. 8. (a) Polarization beat signal of the step-apodized fiber laser before fiber side polishing. (b) Polarization beat signal of the step-apodized fiber laser after fiber side polishing. The insets display the polarization states of the fiber laser visualized on Poincare sphere and the corresponding DOP.

then detected by a high-speed photodetector (PD, Newfocus 1592) with a frequency bandwidth of 3.5 GHz. The heterodyne signal generated by the two arms was monitored with a radio frequency (RF) spectrum analyzer (Rohde & Schwarz FSV4).

Fig. 7(b) shows the resulting heterodyne signal acquired with the DSH method. Moreover, an excellent fit of the measured data (black dots) was carried out by use of a Lorentz curve (red curve), as shown in the inset of Fig. 7(b). The FWHM (i.e., -3 dB linewidth) of the heterodyne signal was 2.6 kHz for the DFB fiber laser output with an output power of 250 μW. However, it should be noted that the 50 km fiber delay line exhibited nonlinear optical effects [28], which could broaden the Gauss spectrum and hide the intrinsic Lorentz linewidth. Hence, the linewidth of the symmetric step-apodized DFB fiber laser should be less than 2.6 kHz.

We also studied the polarization properties of the symmetric step-apodized DFB fiber laser by use two methods. At first, we measured the polarization beat signal using a PD and an RF spectrum analyzer. The laser produced a stable beat frequency of 131.4 MHz with an SNR of 26.9 dB, as shown in Fig. 8(a). It indicates the symmetric step-apodized DFB fiber laser operates in two orthogonal polarization modes. The measured polarization beat frequency corresponds to a fiber birefringence of 7.7×10^{-7}, which is generated by the asymmetric UV exposure during grating inscription and the intrinsic birefringence in the EDF [29], [30]. Subsequently, the polarization state of the symmetric step-apodized DFB fiber laser output was directly observed on Poincare sphere using a polarimeter (Keysight, N7786B), and the degree of polarization (DOP) of the fiber laser was also measured [31]. As shown in the inset of Fig. 8(a), the step-apodized DFB fiber laser exhibits high instability and a low DOP of 0.527 due to the competition between two polarization modes [32]. Therefore, the step-apodized DFB fiber laser operates in unstable two polarization modes.

In addition, the polarization properties of the symmetric step-apodized DFB fiber laser could be altered by means of a fiber side-polishing technique. We used a motor-driven wheel polishing system for side polishing the step-apodized DFB fiber laser and introduced additional birefringence [23], [33]. As a result, the polarization beat signal disappeared in case the symmetric step-apodized DFB fiber laser was side polished to a thickness of 5.1 μm at an input pump power of 40 mW, as shown in Fig. 8(b). It means that the side-polished symmetric step-apodized DFB fiber laser could operate in a single polarization mode. Moreover, as shown in the Poincare sphere in the inset of Fig. 8(b), the side-polished symmetric step-apodized DFB fiber laser exhibits a stable linear polarization with a high DOP of 0.957 and an output power of -29.040 dBm. These results indicate the beat frequency of the DFB fiber laser could be changed due to the change in birefringence,

resulting from the changes in fiber cavity shape and the changes in fiber internal stress distribution. Moreover, side polishing on DFB fiber lasers by a certain thickness will significantly raise the threshold pump power for one polarization mode. Hence, single polarization DFB fiber lasers could be created by using this method.

5. Conclusions

A new method has been demonstrated for fabricating a symmetric step-apodized DFB fiber laser with improved efficiency and a narrow linewidth. This design consists of a weak uniform phase-shifted FBG embedded in a pair of strong FBGs. This design can increase the effective cavity length of DFB fiber laser and improve the fiber laser output efficiency. Moreover, the symmetric step-apodized DFB laser cavity proposed in this work has a phase shift located in the grating center. It could simplify the design process significantly due to the symmetry in laser cavity. The slope efficiency of the proposed symmetric step-apodized DFB fiber laser is 1.06%, which is higher than that of a uniform DFB fiber laser (i.e., 0.45%) under the same cavity length and pump conditions. In addition, the step-apodized DFB fiber laser exhibits a high stability of the fluctuations in lasing wavelength and output power less than 12 pm and 0.13 dB within 24 hours, respectively. Moreover, the step-apodized DFB fiber laser has a narrow linewidth of less than 2.6 kHz, and could operate in dual polarization modes or a stable single polarization mode. As a result, this symmetric step-apodized DFB fiber laser may be developed for use in high-performance optical fiber sensor and coherent optical fiber communication systems.

References

[1] M. Ibsen, S. U. Alam, M. N. Zervas, A. B. Grudinin, and D. N. Payne, "8- and 16-channel all-fiber DFB laser WDM transmitters with integrated pump redundancy," *IEEE Photon. Technol. Lett.*, vol. 11, no. 9, pp. 1114–1116, Sep. 1999.

[2] J. T. Kringlebotn, W. H. Loh, and R. I. Laming, "Polarimetric Er3+-doped fiber distributed-feedback laser sensor for differential pressure and force measurements," *Opt. Lett.*, vol. 21, no. 22, pp. 1869–1871, 1996.

[3] O. Hadeler, E. Rønnekleiv, M. Ibsen, and R. I. Laming, "Polarimetric distributed feedback fiber laser sensor for simultaneous strain and temperature measurements," *Appl. Opt.*, vol. 38, no. 10, pp. 1953–1958, 1999.

[4] F. Zhang, W. Zhang, F. Li, and Y. Liu, "DFB fiber laser hydrophone with band-pass response," *Opt. Lett.*, vol. 36, no. 22, pp. 4320–4322, 2011.

[5] W. Zhang, Y. C. Lai, J. A. R. Williams, C. Lu, L. Zhang, and I. Bennion, "A fibre grating DFB laser for generation of optical microwave signal," *Opt. Laser Technol.*, vol. 32, no. 5, pp. 369–371, 2000.

[6] J. T. Kringlebotn, J. L. Archambault, L. Reekie, and D. N. Rayne, "Er3+:Yb3+ -codoped fiber distributed-feedback laser," *Opt. Lett.*, vol. 19, no. 24, pp. 2101–2103, 1994.

[7] S. Loranger, A. Tehranchi, H. G. Winful, and R. Kashyap, "Realization and optimization of phase-shifted distributed feedback fiber Bragg grating Raman lasers," *Optica*, vol. 5, no. 3, pp. 295–302, 2018.

[8] Q. Li *et al.*, "DFB laser based on single mode large effective area heavy concentration EDF," *Opt. Exp.*, vol. 20, no. 21, pp. 23684–23689, 2012.

[9] M. I. Skvortsov, A. A. Wolf, A. V. Dostovalov, A. A. Vlasov, V. A. Akulov, and S. A. Babin, "Distributed feedback fiber laser based on a fiber Bragg grating inscribed using the femtosecond point-by-point technique," *Laser Phys. Lett.*, vol. 15, 2018, Art. no. 035103.

[10] K. Yelen, M. N. Zervas, and L. M. B. Hickey, "Fiber DFB lasers with ultimate efficiency," *J. Lightw. Technol.*, vol. 23, no. 1, pp. 32–43, Jan. 2005.

[11] A. Melloni, M. Floridi, F. Morichetti, and M. Martinelli, "Equivalent circuit of Bragg gratings and its application to Fabry-Pérot cavities," *J. Opt. Soc. Amer. A*, vol. 20, no. 2, pp. 273–281, 2003.

[12] H. Kogelnik and C. V. Shank, "Coupled-wave theory of distributed feedback lasers," *J. Appl. Phys.*, vol. 43, no. 5, pp. 2327–2335, 1972.

[13] W. H. Loh and R. I. Laming, "1.55 um phase-shifted distributed feedback fiber laser," *Electron. Lett.*, vol. 31, no. 17, pp. 1440–1442, 1995.

[14] S. A. Babin, D. V. Churkin, A. E. Ismagulov, S. I. Kablukov, and M. A. Nikulin, "Single frequency single polarization DFB fiber laser," *Laser Phys. Lett.*, vol. 4, no. 6, pp. 428–432, 2010.

[15] A. D. Guzman-Chávez, Y. O. Barmenkov, and A. V. Kir'yanov, "Spectral dependence of the excited-state absorption of erbium in silica fiber within the 1.48–1.59 μm range," *Appl. Phys. Lett.*, vol. 92, 2008, Art. no. 191111.

[16] Y. O. Barmenkov, A. V. Kiryanov, A. D. Guzman-Chavez, J. L. Cruz, and M. V. Andres, "Excited-state absorption in erbium-doped silica fiber with simultaneous excitation at 977 and 1531 nm," *J. Appl. Phys.*, vol. 106, 2009, Art. no. 083108.

[17] A. V. Kir'yanov, Y. O. Barmenkov, G. E. Sandoval-Romero, and L. Escalante-Zarate, "Er3+ concentration effects in commercial erbium-doped silica fibers fabricated through the MCVD and DND technologies," *IEEE J. Quantum Electron.*, vol. 49, no. 6, pp. 511–521, Jun. 2013.

[18] K. Yelen, L. M. B. Hickey, and M. N. Zervas, "A new design approach for fiber DFB lasers with improved efficiency," *IEEE J. Quantum Electron.*, vol. 40, no. 6, pp. 711–720, Jun. 2004.
[19] S. K. Turitsyn, S. A. Babin, D. V. Churkin, I. D. Vatnik, M. Nikulin, and E. V. Podivilov, "Random distributed feedback fiber lasers," *Phys. Rep.*, vol. 542, no. 2, pp. 133–193, 2014.
[20] M. Yamada and K. Sakuda, "Analysis of almost-periodic distributed feedback slab waveguides via a fundamental matrix approach," *Appl. Opt.*, vol. 26, no. 16, pp. 3474–3478, 1987.
[21] Y. O. Barmenkov, D. Zalvidea, S. Torrespeiró, J. L. Cruz, and M. V. Andrés, "Effective length of short Fabry-Perot cavity formed by uniform fiber Bragg gratings," *Opt. Exp.*, vol. 14, no. 14, pp. 6394–6399, 2006.
[22] J. Zhou *et al.*, "Novel fabrication technique for phase-shifted fiber Bragg gratings using a variable-velocity scanning beam and a shielded phase mask," *Opt. Exp.*, vol. 26, no. 10, pp. 13311–13321, 2018.
[23] K. Guo *et al.*, "Beat frequency tuning in dual-polarization distributed feedback fiber laser using side polishing technique," *Opt. Exp.*, vol. 26, no. 26, pp. 34699–34710, 2018.
[24] T. Erdogan, "Fiber grating spectra," *J. Lightw. Technol.*, vol. 15, no. 8, pp. 1277–1294, Aug. 1997.
[25] Y. O. Barmenkov, A. V. Kir'yanov, P. Perez-Millan, J. L. Cruz, and M. V. Andres, "Threshold of a symmetrically pumped distributed feedback fiber laser with a variable phase shift," *IEEE J. Quantum Electron.*, vol. 44, no. 8, pp. 718–723, Aug. 2008.
[26] T. Okoshi, K. Kikuchi, and A. Nakayama, "Novel method for high resolution measurement of laser output spectrum," *Electron. Lett.*, vol. 16, no. 16, pp. 630–631, 2007.
[27] L. Richter, H. Mandelberg, M. Kruger, and P. Mcgrath, "Linewidth determination from self-heterodyne measurements with subcoherence delay times," *IEEE J. Quantum Electron.*, vol. QE-22, no. 11, pp. 2070–2074, Nov. 1986.
[28] G. P. Agrawal and N. A. Olsson, "Self-phase modulation and spectral broadening of optical pulses in semiconductor laser amplifiers," *IEEE J. Quantum Electron.*, vol. QE-25, no. 11, pp. 2297–2306, Nov. 1989.
[29] A. M. Vengsarkar, Q. Zhong, D. Inniss, W. A. Reed, P. J. Lemaire, and S. G. Kosinski, "Birefringence reduction in side-written photo induced fiber devices by a dual-exposure method," *Opt. Lett.*, vol. 19, no. 16, pp. 1260–1262, 1994.
[30] H. Renner, "Effective-index increase, form birefringence and transition losses in UV-side-illuminated photosensitive fibers," *Opt. Exp.*, vol. 9, no. 11, pp. 546–560, 2001.
[31] J. He *et al.*, "Highly birefringent phase-shifted fiber Bragg gratings inscribed with femtosecond laser," *Opt. Lett.*, vol. 40, no. 9, pp. 2008–2011, 2015.
[32] S. Mo *et al.*, "A 1014 nm linearly polarized low noise narrow-linewidth single-frequency fiber laser," *Opt. Exp.*, vol. 21, no. 10, pp. 12419–12423, 2013.
[33] J. Zhao *et al.*, "Rough side-polished fiber with surface scratches for sensing applications," *IEEE Photon. J.*, vol. 7, no. 3, Jun. 2015, Art. no. 6801107.